

---

---

--

---

---

---

# Contents

<b>Table of Contents</b>	<b>i</b>
<b>List of Figures</b>	<b>i</b>
<b>List of Tables</b>	<b>ii</b>
0.1 Coupling SiV centers to Vertical-Cavity Surface Emitting Lasers . . . . .	1
0.1.1 Vertical-Cavity Surface Emitting Lasers . . . . .	1
0.1.2 SiV center in a Vertical-Cavity Surface Emitting Laser . . . . .	2
<b>Index</b>	<b>9</b>

# List of Figures

1	Sketch of a vertical-cavity surface emitting laser . . . . .	2
2	SEM image of an array of VCSELs . . . . .	3
3	Emission spectra and optical power of VCSEL Bm4 . . . . .	4
4	Scans of VCSELs with and without SiV center . . . . .	5
5	SiV center properties before and after pick-and-place . . . . .	6
6	(a) Scan of the laser light stemming from the VCSEL Bm4 and the fluorescence light from the SiV center in the filter window 730 nm to 750 nm. (b) Scan of the laser light stemming from the VCSEL Bm2 without coupled SiV center. The outcome of the two scans is almost identical. . . . .	7
7	(a) Recorded Spectrum of the SiV center in the transferred nanodiamond on VCSEL Bm4 during VCSEL operation. No distinct SiV center lines are visible. (b) Recorded spectrum of VCSEL Bm2 (without SiV center) . . . . .	8
8	Reflectivity of the Distributed Bragg reflector (DBR) of the VCSEL, and spectrum of the SiV center measured during VCSEL excitation. The reflectivity of the DBR and the VCSEL emission spectra are depicted with different scales. The shape of the measurement of the SiV center during VCSEL operation coincides with the shape of the DBR reflectivity. The spectrum of the SiV center is not visible. As the emission from the SiV center is small compared to the intensity of the laser sideband in the same wavelength regime, the SiV centers emission is not detectable	
	warum schaut das spectrum anders aus als das, was einzeln geplottet ist?	
	. . . . .	8

---

---

# List of Tables

## 0.1 Coupling SiV centers to Vertical-Cavity Surface Emitting Lasers

In the context of metrology, controllable single photon sources, operating at room temperature, are an extremely important prospect. Such devices are anticipated to play a key role in the development and calibration of detectors and measurement methods aiming to resolve optical flux down to single-photon resolution [?]. As such single photon source form a cornerstone of the efforts directed towards the redefinition of the candela in terms of single photons, see discussion in ??.

Here we attempt to create a hybrid-integrated single photon source by placing a nanodiamond ideally containing a solitary SiV centers on top of a vertical-cavity surface emitting lasers (VCSELs). The SiV center is situated such that output laser of the VCSEL can be used to optically excite the color center. Since the VCSEL laser can be controlled very well, SiV center operation can be steered reliably. Through the use of suitable optical filters allowing only SiV center fluorescence light to emerge, a controlled single photon source can be realized in principle.

In the following we give a short discussion of VCSELs. Next we discuss the coupling of SiV centers to VCSELs and report on the optical properties of the resulting hybrid-integrated light source.

### 0.1.1 Vertical-Cavity Surface Emitting Lasers

A vertical-cavity surface emitting laser is a type of semi-conductor laser diode [?, ?, ?]. Figure 1 illustrates a common design consisting of a  $p$ -layer on top and a  $n$ -layer at the bottom separated by a so-called active area. When a current is applied across the device, charge carriers migrate towards the active region. Holes act as charge carriers in the  $p$  region, whilst electrons carry charge in the  $n$ -region. The material properties of the active region is chosen such that when electrons and holes spontaneously recombine, a photon is emitted in the process. Electron-hole pairs can also dissipated via the creation of phonons leading to losses in the form of heat. To define the region for recombination to occur and to control the optical properties of the device, additional thin layers of semiconducting material can be introduced in the active area. These result in the formation of quantum wells with associated energy levels and resulting preferred transitions with well-defined energies for the recombination of electrons and holes.

To achieve lasing, stimulated recombination and thus stimulated emission of photons is required. To facilitate this both  $p$ -region and  $n$ -region are constructed in a layered fashion allowing them to act as highly-efficient distributed Bragg reflectors (DBR). Thus the active region is sandwiched by two mirrors forming the resonator of the laser diode. Spontaneously emitted photons thus are temporarily trapped continuously interacting with the active region. Provided the presence of sufficient electron-hole pairs, a photon can stimulate their recombination and thus the emission of further identical photons which themselves increase the stimulated emission. If enough identical photons are gained in this process, a coherent laser beam is formed by the fraction of photons escaping the resonator through the  $p$ -region. As a result the laser beam produced by a VCSEL is perpendicular to the substrate it resided on.

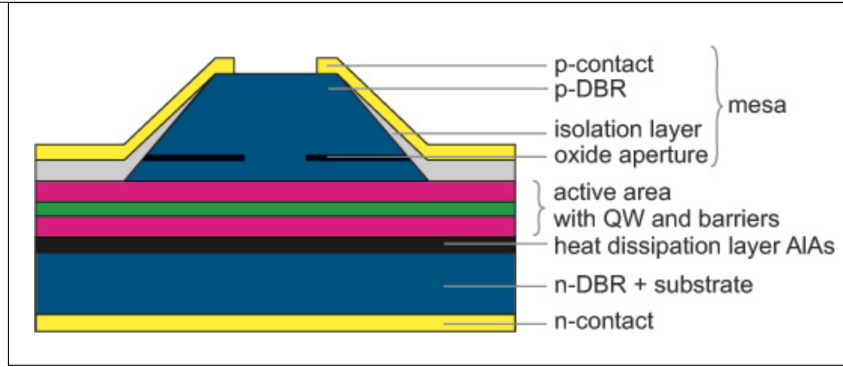


Figure 1: Illustration of a VCSEL laser diode [?]. When a current is applied across the device via contacts (yellow), holes and electrons migrate from the  $p$ -region (blue, top) and the  $n$ -region (blue, bottom) towards the active region (purple+green, center) where they recombine emitting photons. A quantum well is inserted in the active region, shaping the recombination process.  $p$ -region and  $n$ -region are acting as DBRs forming the resonator of the laser. When enough photons are gained by via stimulated emission, a laser beam emerges from the  $p$ -region after passing an oxide aperture.

VCSELs have a range of properties that make them particularly interesting for industrial applications such low power consumption, ease of fabrication and cheap production. As a result, VCSELs are utilized in a broad range of applications including fiber optic communications or precision sensing and are used widely in commonly encountered devices such as computer mice or laser printers [?].

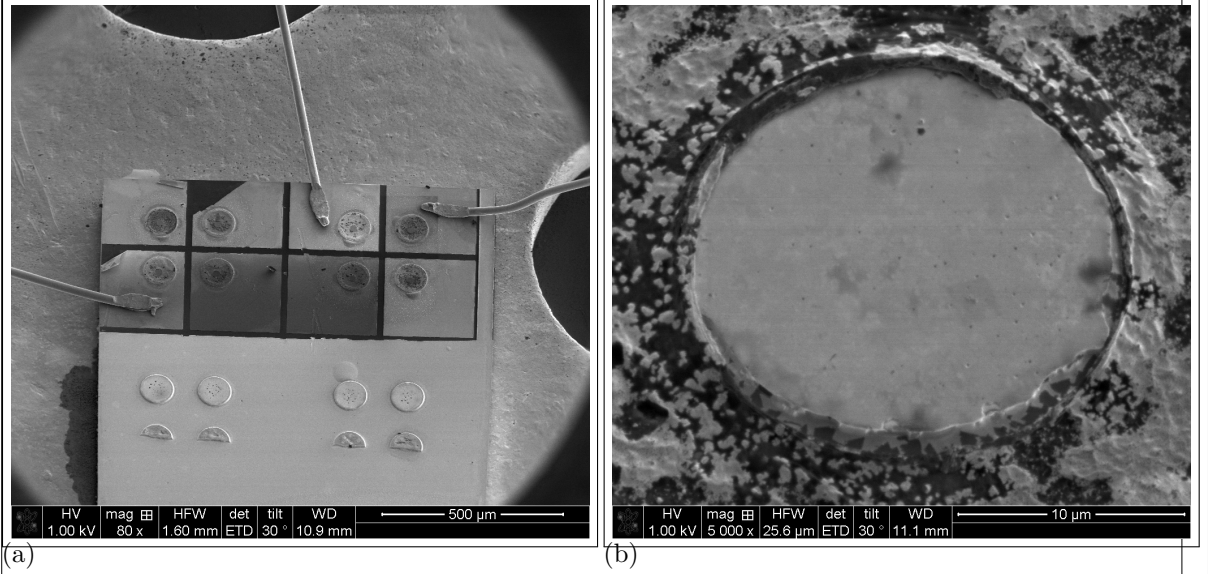
In the context of this thesis VCSELs offer several advantages. Their output beam is perpendicular to the substrate surface and suitable to excite SiV centers. This means that nanodiamonds containing SiV centers can simply be placed ontop of the device. Furthermore their physical size is ideal for the nanodiamonds we work with. The small size of VCSELs will make it easier to deploy the resulting hybrid-integrated light sources in future applications.

### 0.1.2 SiV center in a Vertical-Cavity Surface Emitting Laser

To conduct our research, we recieved an array of red AlGaInP-based oxide-confined VCSELs from P. Michler, Stuttgart University. The array includes three individually operable VCSELs, two of which, labeled VCSEL Bm4 and VCSEL Bm2 were used in our experiments, see Figure 2a.

The VCSELs we obtained use a  $n$ -type DBR consisting of 50 pairs of AlAs/ $\text{Al}_{0.5}\text{Ga}_{0.5}\text{As}$  mirror pairs while the  $p$ -type DBR is formed by 36  $\text{Al}_{0.95}\text{Ga}_{0.05}\text{As}/\text{Al}_{0.5}\text{Ga}_{0.5}\text{As}$  [?]. The active region itself consists of 4 GaInP quantum wells. An oxide aperture in a field node of the standing wave serves as a spatial filter for maximum modal gain by confining the current and the optical mode. The active diameter which is defined by the oxide aperture is  $5.8\text{ }\mu\text{m}$ .

The available VCSELs are perfect candidates for the excitation of SiV centers in a hybrid integrated single photon source for several reasons. They exhibit a circular beam profile, have low divergence angel and emit linearly polarized light. Their physcial size and the fact, that their output beam is perpendicular to the substrate implies that our nanodiamonds containing



nanodiamonds can simply be placed on top of the structure light-emitting region using pick-and-place methods, see Figure 2b. Thus the VCSELs output laser can be used to optically excite SiV centers.

As a first step towards using VCSELs to excite color centers, we characterized the behaviour of VCSEL Bm4. To this end we operated it at currents of 1.5 mA and 3 mA and recorded the resulting lasing wavelength. The emission spectra showed that the emitted continuous wave laser light to be around 655 nm in wavelength for both currents, see Figure 3a. Previous research within the authors group recorded SiV center intensity maxima at excitation wavelengths of 720 nm and 680 nm [?], aligning reasonably well with the output wavelength of VCSEL Bm4.

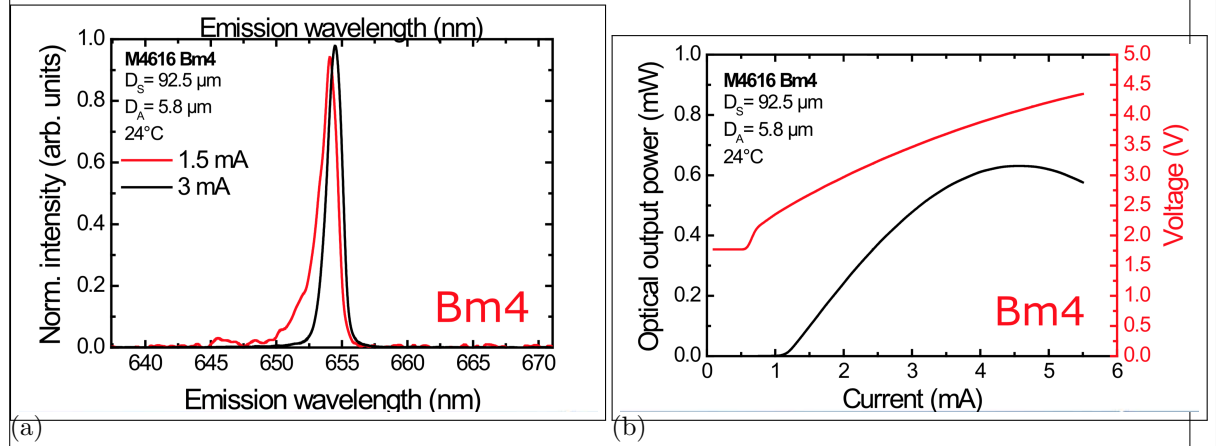


Figure 3: (a) Emission spectrum of VCSEL Bm4 at two different currents. (b) Optical output power and voltage of VCSEL Bm4 in dependence of input current. []

The optical output power of VCSEL Bm4 as a function of the current applied is given in Figure 3b. In addition, the resulting voltages are shown. It can be seen that the maximum power of  $\approx 0.6$  mW is reached for moderate currents of  $\approx 4.5$  mA. While the available optical powers are small comparable to using a conventional laser, low powers are sufficient for initial explorations.

The next step consists of selecting a suitable nanodiamond containing an SiV center followed by transferring it on top of VCSEL Bm4. To this end nanodiamonds 200 nm in size were grown with the CVD method in an iridium coated silicon wafer. We refer the reader to ?? for details on the process.

Next, using the confocal setup described in ?? a nanodiamond was identified exhibiting one dominant line at 746.0 nm with a linewidth of 1.9 nm. Its position on the substrate was determined consecutively using a white light laser scan as described in ?. Given the position of the nanodiamond it was then transferred to VCSEL Bm4 and placed precisely in its active, i.e. light-emitting region. The process of introducing an SiV center to another structure is referred to as coupling.

After successful transfer VCSEL Bm4 was inserted into the confocal setup. Using the laser from the confocal setup we checked if the pick-and-place process caused any modification of the spectroscopic properties of the SiV center such as a decrease of count rate or a modification of the fluorescence light spectrum. During these checks, the VCSEL itself was not active.



As a first check, we scanned the VCSEL surface in an attempt to detect the activity of the introduced SiV center. Figure 4a shows the SiV center as a bright dot in the aperture of VCSEL Bm4. For comparison, a Vertical-Cavity Surface Emitting Laser without coupled SiV center exhibits solely background counts which is shown in Figure 4b.

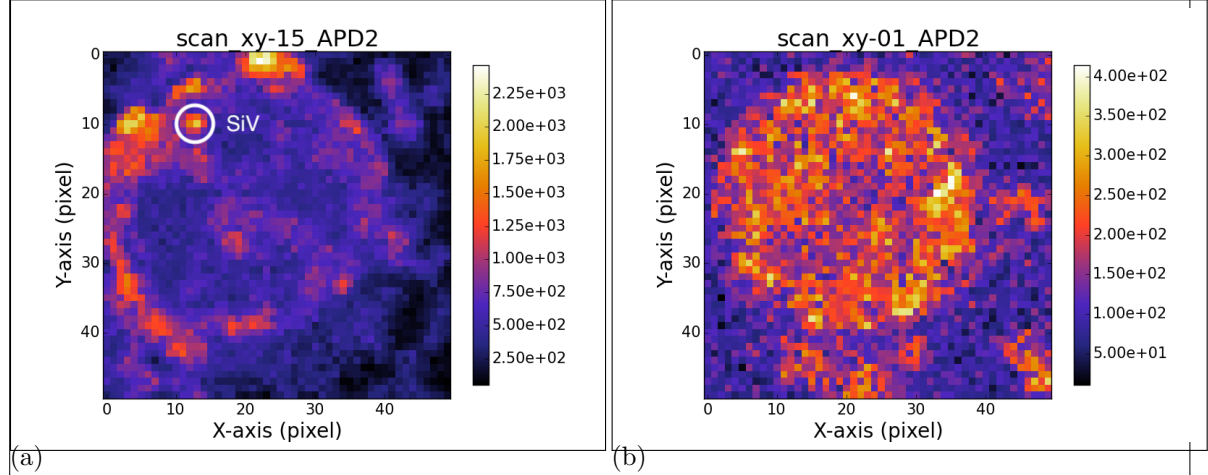


Figure 4: (a) Scan of the VCSEL Bm4 with coupled nanodiamond under excitation with the laser from the confocal setup. The big visible ring is the edge of the circular aperture in the  $p$ -contact of VCSEL Bm4. The bright spot in the upper left corner corresponds to the transferred nanodiamond containing an SiV center causing a spike in the count rate. (b) Scan of the VCSEL Bm2 lacking a nanodiamond under excitation with the laser from the confocal setup. The circular aperture in the  $p$ -contact exhibits a constant count rate. Note the different scales.

The spectrum of the SiV center in the transferred nanodiamond was investigated before and after the pick-and-place process. section 5 shows that the original spectrum before nanodiamond transfer exhibits one dominant line at 746.0 nm, denoted line  $A$ . Furthermore, two minor peaks can be seen. The lower wavelength peak is denoted as line  $B$ . Interestingly, after the pick-and-place process, a different picture emerges shown in section 5. The once dominant line  $A$  is strongly reduced. The new dominant feature is line  $B$ . Note that the count rate of line  $B$  remained the same before and after pick-and-place.

The observed reduction of the intensity of line  $A$  is difficult to explain. One cause could be damage to the color center due to the electron radiation it was exposed to during the pick-and-place process. This is supported by previous research in this authors group recording reduced fluorescence light intensities after color centers were exposed to electron radiation [?]. However, the fact that line  $B$  remains virtually the same before and after pick-and-place is curious, raising the question whether damage alone is sufficient to explain the observed effect. As it stands, the question remains open and is thus subject to further investigation.

With line  $B$  as remaining dominant line we then operated VCSEL Bm4 at 1.84 mA and 3.3 V, turning off the laser of the confocal setup. Thus SiV center excitation is due to the output laser of VCSEL Bm4.

For comparison, we scanned both the surface of VCSEL Bm4 including the nanodiamond as well as VCSEL Bm2 without a nanodiamond. A filter window allowing light between 730 nm to 750 nm was used to allow wavelengths relevant to SiV center emission to pass selectively.

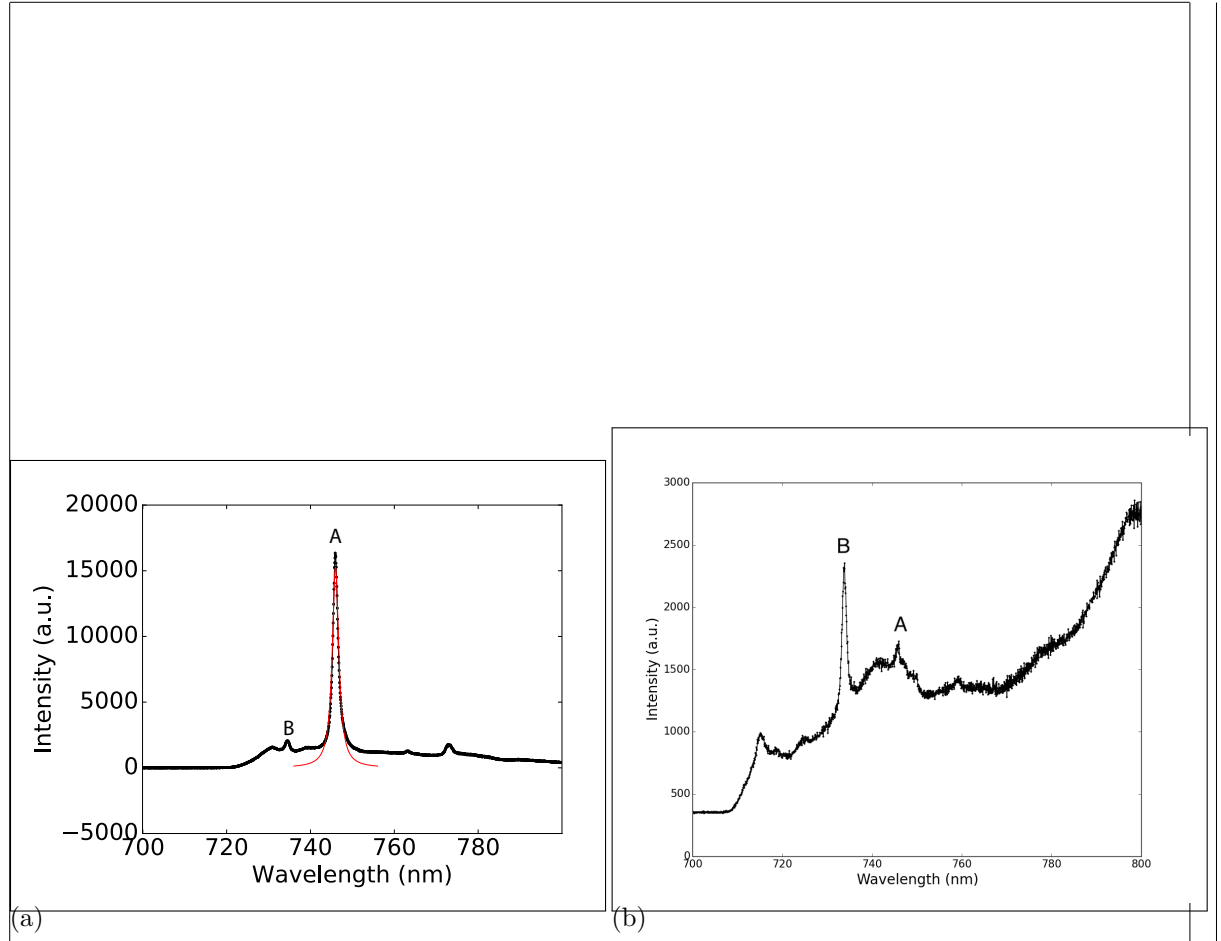


Figure 5: (a) Spectrum of the preselected diamond for transfer onto VCSEL Bm4 before pick-and-place. The strong line denoted *A* exhibits a center wavelength of 746.0 nm and a linewidth of 1.9 nm. Line *B* exhibits a center wavelength of 0 nm and a linewidth of 0 nm

put in correct numbers

(b) Spectrum of the same SiV center after pick-and-place, excited with the same laser as before. While Line *A* is almost gone, line *B* still exists seemingly unchanged and has become the predominant line of the spectrum. We remark that due to material restrictions, different longpass filters were used for the two measurements. Measurement (a) was performed with a 720 nm longpass filter, measurement (b) with a 710 nm longpass filter.

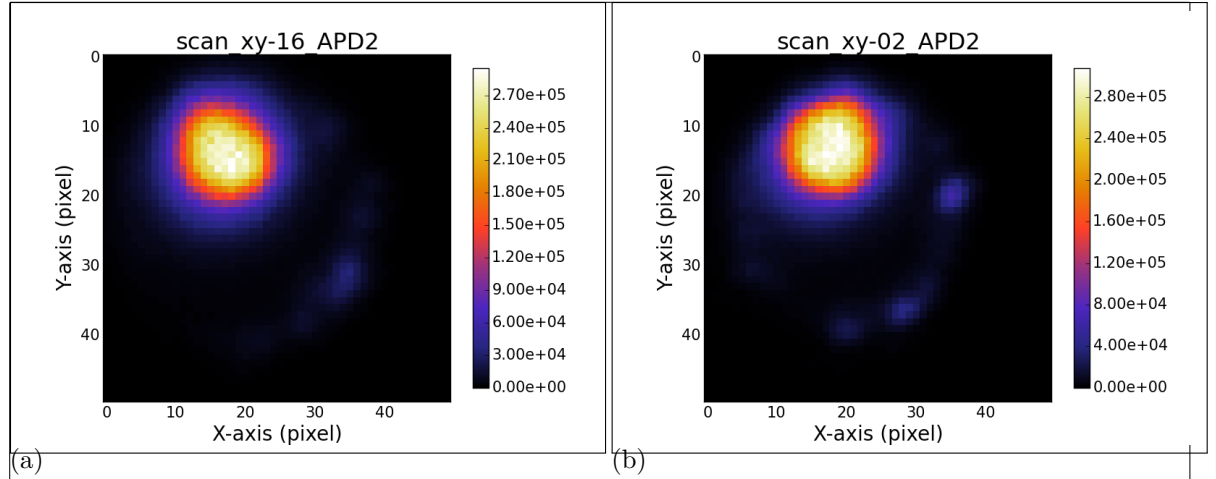


Figure 6: (a) Scan of the laser light stemming from the VCSEL Bm4 and the fluorescence light from the SiV center in the filter window 730 nm to 750 nm. (b) Scan of the laser light stemming from the VCSEL Bm2 without coupled SiV center. The outcome of the two scans is almost identical.

We scanned both the surface of (with nanodiamond) and of VCSEL Bm2 (without nanodiamond) with a 730 nm to 750 nm bandpass filter. This filter window suppresses the VCSEL laser line at 655 nm (3a) while leaving the SiV center emission nearly unchanged. The light areas in ?? correspond to the laser output areas. We measured a spectrum at the same points as before VCSEL operation. In the case of VCSEL Bm4, this spot corresponds to the position of the SiV center. The following observations are made from the measurements:

- In both scans, the laser output area is visible as a big bright spot. There is no difference in intensity between VCSEL Bm4 and Bm2.
- The spectra of VCSEL Bm4 and Bm2 are almost identical.

As diamond material we used CVD grown nanodiamonds. They had been grown on an iridium coated silicon wafer (see ??). These nanodiamonds exhibit a nominal size of 200 nm. First, we selected a nanodiamond which exhibited one dominant line at 746.0 nm with a linewidth of 1.9 nm. Consecutively, its position on the substrate was determined using a white light laser scan as described in ?. It was then transferred to the VCSEL Bm4 described in ?. After a successful transfer of the pre-selected nanodiamond onto the active area of VCSEL Bm4, the VCSEL was put in the confocal setup. Using the laser from the confocal setup we checked if the pick-and-place process caused any modification of the spectroscopic properties of the SiV center such as a decrease of count rate or a modification of the fluorescence light spectrum. For this, the VCSEL itself was not operated itself. First, the VCSEL surface was scanned ?. . A bright dot exhibiting a count rate of a few thousand counts per second is visible where the nanodiamond containing an SiV was put. A comparative scan of a VCSEL without nanodiamond only exhibits a background count rate, as expected (??).

The spectrum of the SiV center in the transferred nanodiamond was investigated before and after the pick-and-place process (??). The original spectrum before nanodiamond transfer exhibits a sharp line at 746.0 nm (denoted line A). After the pick-and-place process, this line is still there, albeit with a low intensity. Another line at 0 nm (denoted line B) which was a minor feature in the spectrum before pick-and-place, is the predominant line after the

was it  
single?

check  
number

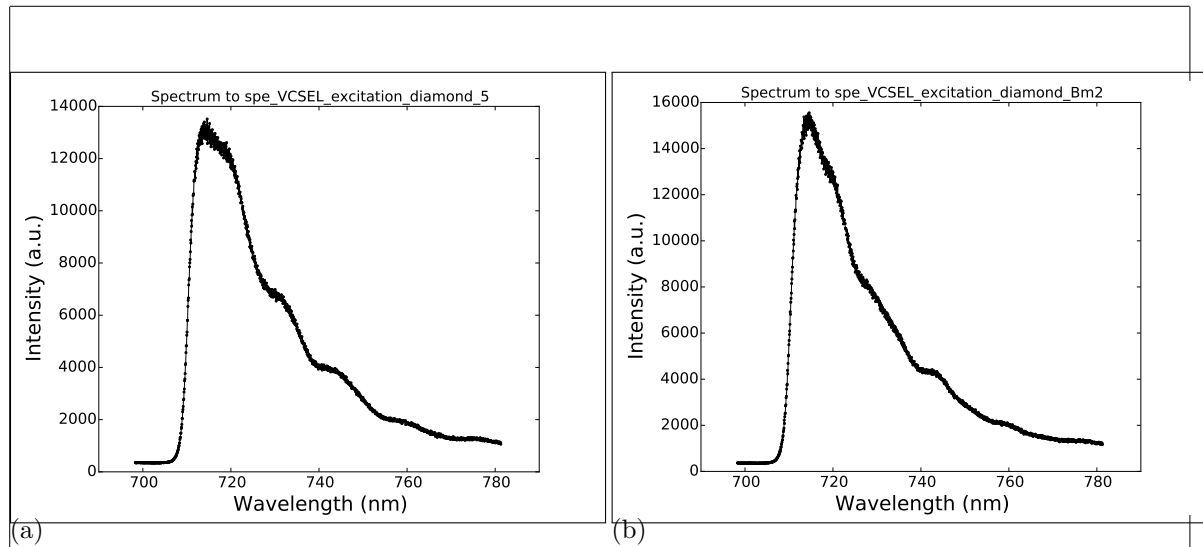


Figure 7: (a) Recorded Spectrum of the SiV center in the transferred nanodiamond on VCSEL Bm4 during VCSEL operation. No distinct SiV center lines are visible. (b) Recorded spectrum of VCSEL Bm2 (without SiV center)

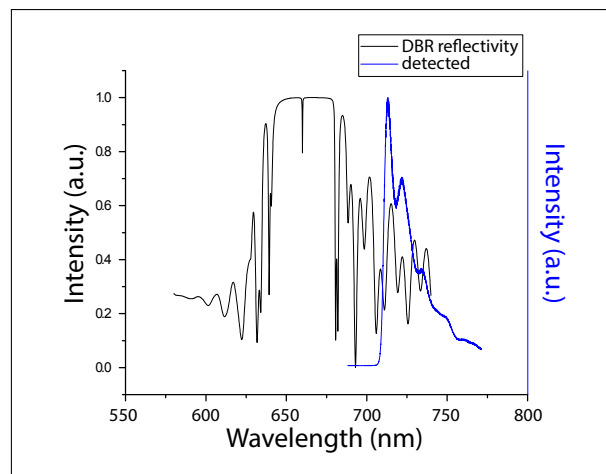


Figure 8: Reflectivity of the Distributed Bragg reflector (DBR) of the VCSEL, and spectrum of the SiV center measured during VCSEL excitation. The reflectivity of the DBR and the VCSEL emission spectra are depicted with different scales. The shape of the measurement of the SiV center during VCSEL operation coincides with the shape of the DBR reflectivity. The spectrum of the SiV center is not visible. As the emission from the SiV center is small compared to the intensity of the laser sideband in the same wavelength regime, the SiV centers emission is not detectable

warum schaut das spectrum anders aus als das, was einzeln geplottet ist?

process. This modification of the spectrum is caused by a reduction of the intensity of line A and constant intensity of line B. The reduction of the intensity of line A may be caused by damage of the color center due to electron radiation. While the energy of the electrons is low compared to the ionization energy of the color center, we observed a reduction of fluorescence light intensity after electron radiation (for a detailed description of this effect, refer to [?]). We then operated the VCSEL at 1.84 mA and 3.3 V and turned off the laser of the confocal setup. We scanned both the surface of VCSEL Bm4 (with nanodiamond) and of VCSEL Bm2 (without nanodiamond) with a 730 nm to 750 nm bandpass filter. This filter window suppresses the VCSEL laser line at 655 nm (3a) while leaving the SiV center emission nearly unchanged. The light areas in ?? correspond to the laser output areas. We measured a spectrum at the same points as before VCSEL operation. In the case of VCSEL Bm4, this spot corresponds to the position of the SiV center. The following observations are made from the measurements:

- In both scans, the laser output area is visible as a big bright spot. There is no difference in intensity between VCSEL Bm4 and Bm2.
- The spectra of VCSEL Bm4 and Bm2 are almost identical.

The spectrum recorded in the confocal setup corresponds well with the DBR reflectivity (??). Hence, we conclude, that the detected emission is due to the VCSEL and does not stem from the SiV center. From these observations, we draw the conclusion that the fluorescence light emission from the SiV center is small compared to the sideband of the VCSEL emission in the wavelength regime where the SiV center emission is expected. Therefore, the SiV center emission is not detectable during VCSEL excitation.

Ongoing work is performed to reduce sideband emission of the VCSEL in the SiV center emission regime. A promising approach is to add a gold layer on top of the VCSEL which acts as a tunable mirror. While films of gold have a transmittance maximum at 500 nm, the transmittance minimum depends on the film's thickness [?]. Hence the goal is to apply a gold film which suppresses the laser sideband in the SiV center emission regime.

In this chapter we showed successful transfer of a nanodiamond containing an SiV center. While the SiV center spectrum was modified after the pick-and-place process, it was clearly identified with the preselected SiV center. Further research has to be performed to enhance the VCSEL emission properties.

numbers

besser  
begründen,  
was passiertev besser  
begründen